Thermosolutal Convection during Dendritic Solidification of Alloys: Part II. Nonlinear Convection

J.C. HEINRICH, S. FELICELLI, P. NANDAPURKAR, and D.R. POIRIER

A mathematical model of thermosolutal convection in directionally solidified dendritic alloys has been developed that includes a mushy zone underlying an all-liquid region. The model assumes a nonconvective initial state with planar and horizontal isotherms and isoconcentrates that move upward at a constant solidification velocity. The initial state is perturbed, nonlinear calculations are performed to model convection of the liquid when the system is unstable, and the results are compared with the predictions of a linear stability analysis. The mushy zone is modeled as a porous medium of variable porosity, consistent with the volume fraction of interdendritic liquid that satisfies the conservation equations for energy and solute concentrations. Results are presented for systems involving lead-tin alloys (Pb-10 wt pct Sn and Pb-20 wt pct Sn) and show significant differences with results of plane-front solidification. The calculations show that convection in the mushy zone is mainly driven by convection in the all-liquid region, and convection of the interdendritic liquid is only significant in the upper 20 pct of the mushy zone if it is significant at all. The calculated results also show that the systems are stable at reduced gravity levels of the order of $10^{-4}\ g_0$ ($g_0 = 980\ \text{cm} \cdot \text{s}^{-1}$) or when the lateral dimensions of the container are small enough, for stable temperature gradients between $2.5 \leq G_L \leq 100\ \text{K} \cdot \text{cm}^{-1}$ at solidification velocities of 2 to 8 $\text{cm} \cdot \text{h}^{-1}$.

I. INTRODUCTION

DURING dendritic solidification of alloys, liquid flow is induced both by buoyancy forces and solidification shrinkage. Based on the experimental base of several investigators (*e.g.*, Laxmanan *et al.*,[1] Sarazin and Hellawell,[2] and Streat and Weinberg,[3]), there is strong evidence that the major reason for liquid flow is often the former, *i.e.*, thermosolutal convection. This can be seen in Figure 1, which shows schematically the variation of the concentration of solute *vs* distance from the base of a directionally solidified ingot.

Two curves are shown in Figure 1. One shows macrosegregation when thermosolutal convection is absent and flow of the interdendritic liquid is induced primarily by solidification shrinkage. This results in a positive segregation at the surface of the solidified ingot, which is often deemed "inverse segregation."[4] On the other hand, when thermosolutal convection occurs, there is apparently an advection of solute from the enriched mushy zone to the all-liquid zone that results in negative segregation at the surface and a gradual increase of the solutal concentration in the completely solidified ingot.

The major emphasis of this paper is to model the thermosolutal convection responsible for the latter type of macrosegregation described above. In an accompanying paper,[5] the thermosolutal convection was analyzed in terms of its linear stability. As a model system, Pb-20 wt pct Sn alloy solidifying at $0.002\ \text{cm} \cdot \text{s}^{-1}$ was selected. Marginal stability curves, in terms of the thermal gradient at the dendrite tips *vs* the horizontal wave number of the perturbed variables, were calculated for gravitational constants of g_0, $0.5\ g_0$, $0.1\ g_0$, and $0.01\ g_0$. For $0.0001\ g_0$, the system was found by calculation to be stable for all thermal gradients ($2.5 \leq G_L \leq 100\ \text{K} \cdot \text{cm}^{-1}$) and for all wave numbers ($0 \leq \omega \leq 130\ \text{cm}^{-1}$). For the greater fractions of g_0, however, there were no minima in the marginal stability curves, so that the system was not found to be unconditionally stable for all wave numbers. The analyses did reveal that there are probable container widths, below which convection can be suppressed.

In this paper, the same type of a system is formulated using dimensionless variables. Calculations are presented for various situations in which the linear stability analyses have predicted convection and no convection,[5] respectively. The nonlinear calculations presented herein agree with the predictions of the linear stability analyses. It is important to note, however, that the present nonlinear analysis does not permit the volume fraction of liquid in the mushy zone to deviate from its distribution determined for the nonconvecting and steady state. While this is a reasonable assumption to make for convection near the critical state, and it permits a prediction of the conditions in which thermosolutal convection is expected, such an assumption does not allow an investigation of the supercritical stage of convection that leads to the formation of localized segregates that are sometimes called "channel segregates" or "freckles."[2] In future work, we intend to model the supercritical convection and the formation of channel segregates by relaxing the assumption that the volume fraction of liquid in the mushy zone does not vary with time.

II. MATHEMATICAL MODEL

A. *Conservation Equations*

The physical situation is illustrated by Figure 2. We assume that a binary alloy solidifies vertically in a two-dimensional strip of width W. In Figure 2, S denotes

J.C. HEINRICH, Associate Professor, and S. FELICELLI, Graduate Student, are with the Department of Aerospace and Mechanical Engineering and P. NANDAPURKAR, Research Associate, and D.R. POIRIER, Professor, are with the Department of Materials Science and Engineering, The University of Arizona, Tucson, AZ 85721.

Manuscript submitted January 11, 1989.

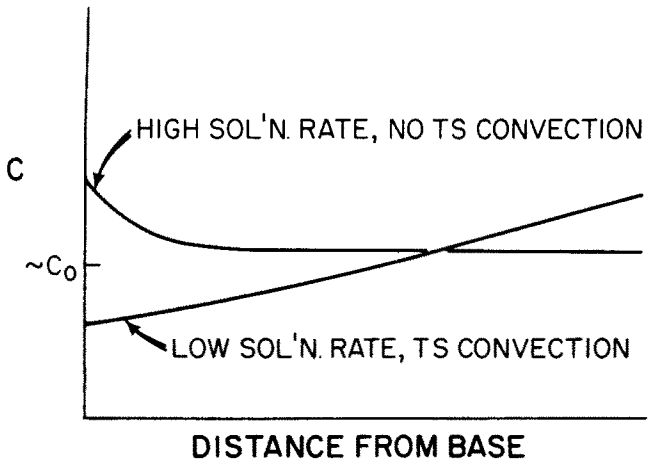

Fig. 1—Variation of solute concentration *vs* distance from the base with and without thermosolutal convection for a directionally solidified ingot.

the all-solid zone, L the all-liquid zone, and $L + S$ the mushy zone. The coordinate system is located at $z = 0$ and moves upward at the constant solidification velocity, V.

In Part I[5] of this paper, all of the major assumptions are listed. We start with Eqs. [6] through [9] of Nandapurkar *et al.*[5] for the conservation equations written for the moving coordinate system and in a dimensional form.

(mass conservation)

$$\frac{\partial u}{\partial x} + \frac{\partial w}{\partial z} = 0 \qquad [1]$$

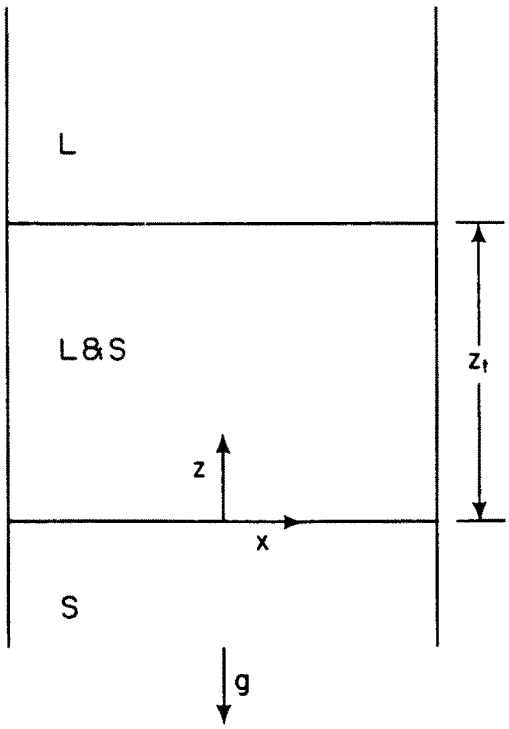

Fig. 2—Geometry and coordinate system for directional solidification of a dendritic alloy.

(x momentum)

$$\frac{\partial u}{\partial t} - V\frac{\partial u}{\partial z} + \frac{1}{\phi}\left(u\frac{\partial u}{\partial x} + w\frac{\partial u}{\partial z}\right) = -\frac{\phi}{\rho_0}\frac{\partial p}{\partial x} + \nu_0\nabla^2 u - \nu_0\frac{\phi}{K}u \qquad [2]$$

(z momentum)

$$\frac{\partial w}{\partial t} - V\frac{\partial w}{\partial z} + \frac{1}{\phi}\left(u\frac{\partial w}{\partial x} + w\frac{\partial w}{\partial z}\right) = -\frac{\phi}{\rho_0}\frac{\partial p}{\partial z} + \nu_0\nabla^2 w - \nu_0\frac{\phi}{K}w - \phi\frac{\rho}{\rho_0}g \qquad [3]$$

(energy)

$$\frac{\partial T}{\partial t} + u\frac{\partial T}{\partial x} + (w - V)\frac{\partial T}{\partial z} = \bar{\alpha}\nabla^2 T + \frac{VL}{\hat{c}}\frac{d\phi}{dz} \qquad [4]$$

and

(solute)

$$\phi\frac{\partial C}{\partial t} + u\frac{\partial C}{\partial x} + (w - \phi V)\frac{\partial C}{\partial z} = D\left[\phi\nabla^2 C + \frac{\partial C}{\partial z}\frac{d\phi}{dz}\right] + (1 - k)V\frac{d\phi}{dz}C \qquad [5]$$

In the equations for momentum, u and w are the components of superficial velocity, ρ_0 is the density of the liquid at the reference state with a concentration C_∞ and liquidus temperature T_0, p is pressure, ν_0 is the kinematic viscosity of the liquid at the reference state, K is the permeability, g is the gravitational acceleration, and ρ is the variable density of the liquid. The permeability is that recommended for a mushy zone with a columnar dendritic structure:[6]

$$K = ad_1^2\frac{\phi^3}{(1 - \phi)} \qquad [6]$$

where d_1 is the primary dendrite arm spacing, ϕ is the local fraction of liquid, and a is a constant. The variable density for the Boussinesq term in Eq. [2] is expressed in the usual manner:

$$\rho = \rho_0[1 - \beta_T(T - T_0) - \beta_C(C - C_\infty)] \qquad [7]$$

where β_T is the thermal expansion coefficient, β_C is the solutal expansion coefficient, and T is the temperature.

In the energy equation, $\bar{\alpha} = \kappa/(\rho_0\hat{c})$, where κ and $\hat{c}$ are the thermal conductivity and heat capacity, respectively, within the mushy zone, and L is the latent heat of fusion. In the solute equation, D is the diffusivity of the solute in the liquid, and k is the equilibrium partition ratio. It is also assumed that $\phi = \phi(z)$ in the moving coordinate system.

Equations [1] through [5] and Eq. [7] apply both to the mushy zone and to the all-liquid zone. Specifically, with the volume fraction of liquid, ϕ, equal to one, the permeability is infinity, and the Darcy terms of the component momentum equations (Eqs. [2] and [3]) become zero. Hence, the component equations for momentum

reduce to the usual Navier-Stokes equations with the Boussinesq approximation. The energy and solutal conservation equations (Eqs. [4] and [5]) also reduce to the usual forms for the single-phase fluids when ϕ is unity. Thus, we are assured of continuity in the major variables and their derivatives in the transition from the mushy zone to the all-liquid zone.

We now rewrite Eqs. [1] through [5] with nondimensional quantities.

(1) The thermal Rayleigh number is

$$\mathrm{Ra}_T = \frac{g\beta_T G_L H^4}{\nu_0 \bar{\alpha}} \qquad [8]$$

where G_L is the specified initial thermal gradient at the tip of the dendrites and H is a characteristic length. For these nonlinear calculations, we have selected $H = z_t$, the height of the mushy zone.

(2) The solutal Rayleigh number is

$$\mathrm{Ra}_C = \frac{g\beta_C C_\infty H^3}{\nu_0 D} \qquad [9]$$

where C_∞ is the concentration of solute in the bulk liquid.

(3) The Prandtl number is

$$\mathrm{Pr} = \nu_0/\bar{\alpha} \qquad [10]$$

(4) The Schmidt number is

$$\mathrm{Sc} = \nu_0/D \qquad [11]$$

(5) The Darcy number is

$$\mathrm{Da} = K/H^2 \qquad [12]$$

(6) The reference velocity is

$$U = (g\beta_T G_L H^2)^{1/2} \qquad [13]$$

(7) The nondimensional interface velocity is

$$\hat{V} = V/U \qquad [14]$$

The momentum diffusion time scale

$$\tau = \frac{H^2}{\nu_0} \qquad [15]$$

has been chosen because it lies between the temperature and solute diffusion time scales. The temperature and solute concentrations are nondimensionalized according to

$$T = \frac{T' - T_0}{G_L H} \qquad [16]$$

and

$$C = \frac{C' - C_\infty}{C_\infty} \qquad [17]$$

respectively, where the prime denotes a dimensional quantity and T_0 is the liquidus temperature of the alloy with concentration C_∞. For reference pressure, we choose

$$P = \rho_0 H^2/\tau^2 \qquad [18]$$

Finally, the nondimensional components of velocity are

$$u = u'/U \quad \text{and} \quad w = w'/U \qquad [19a,b]$$

The nondimensional coordinates are

$$x = x'/H \quad \text{and} \quad z = z'/H \qquad [20a,b]$$

Nondimensional time is

$$t = t'/\tau \qquad [21]$$

And nondimensional pressure is

$$p = p^*/P \qquad [22]$$

Notice that in the definition of the nondimensional pressure, a dimensional pressure p^* is introduced. The dimensional pressure gradient in Eqs. [1] and [2] is written as $\nabla p' = \nabla p_s + \nabla p^*$, where $\nabla p_s = -\rho_0 g$, so that p^* satisfies $\nabla p^* = \nabla p' + \rho_0 g$.

Because the equations in the mushy zone reduce to the equations in the liquid when $\phi = 1$, the whole system can be described by one set of equations. In nondimensional form, Eqs. [1] through [5] become

$$\frac{\partial u}{\partial x} + \frac{\partial w}{\partial z} = 0 \qquad [23]$$

$$\frac{\partial u}{\partial t} + \left(\frac{\mathrm{Ra}_T}{\mathrm{Pr}}\right)^{1/2}\left[\left(\frac{w}{\phi} - \hat{V}\right)\frac{\partial u}{\partial z} + \frac{u}{\phi}\frac{\partial u}{\partial x}\right] = -\phi\left(\frac{\mathrm{Pr}}{\mathrm{Ra}_T}\right)^{1/2}\frac{\partial p}{\partial x} + \nabla^2 u - \frac{\phi}{\mathrm{Da}}u \qquad [24]$$

$$\frac{\partial w}{\partial t} + \left(\frac{\mathrm{Ra}_T}{\mathrm{Pr}}\right)^{1/2}\left[\left(\frac{w}{\phi} - \hat{V}\right)\frac{\partial w}{\partial z} + \frac{u}{\phi}\frac{\partial w}{\partial x}\right] = -\phi\left(\frac{\mathrm{Pr}}{\mathrm{Ra}_T}\right)^{1/2}\frac{\partial p}{\partial z} + \nabla^2 w - \frac{\phi}{\mathrm{Da}}w + \phi\left(\frac{\mathrm{Ra}_T}{\mathrm{Pr}}\right)^{1/2}\left[T + \frac{\mathrm{Ra}_C \mathrm{Pr}}{\mathrm{Ra}_T \mathrm{Sc}}C\right] \qquad [25]$$

$$\frac{\partial T}{\partial t} + \left(\frac{\mathrm{Ra}_T}{\mathrm{Pr}}\right)^{1/2}\left\{u\frac{\partial T}{\partial x} + (w - \hat{V})\frac{\partial T}{\partial z}\right\} = \frac{1}{\mathrm{Pr}}\nabla^2 T + \left(\frac{\mathrm{Ra}_T}{\mathrm{Pr}}\right)^{1/2}\frac{\hat{V}L}{\hat{c}G_L H}\frac{d\phi}{dz} \qquad [26]$$

$$\phi\frac{\partial C}{\partial t} + \left(\frac{\mathrm{Ra}_T}{\mathrm{Pr}}\right)^{1/2}\left(u\frac{\partial C}{\partial x} + (w - \phi\hat{V})\frac{\partial C}{\partial z}\right) = \frac{1}{\mathrm{Sc}}\left[\phi\nabla^2 C + \frac{\partial C}{\partial z}\frac{d\phi}{dz}\right] + \left(\frac{\mathrm{Ra}_T}{\mathrm{Pr}}\right)^{1/2}\hat{V}(1-k)\frac{d\phi}{dz}(1 + C) \qquad [27]$$

B. *The Initial State*

We assume that initially there is no convection and that, in the mushy zone, Eqs. [21] through [25] of Nandapurkar *et al.*[5] describe C, T, and ϕ. The nonconvecting state is specified by inputting G_L, V, and C_∞ with

$$\phi(x, z_t, 0) = 1$$

$$\phi(x, 0, 0) \geq 0$$

and

$$T'(x, 0, 0) = T'_E$$

In addition to obtaining C, T, and ϕ in the nonconvecting mushy zone, the position of the dendrite tips, z_t, is also obtained as part of the solution.

The characteristic length, H, is made equal to z_t, and the height of the all-liquid zone is also made equal to $H = z_t$. The temperature at the top of the all-liquid zone simply becomes

$$T'_H = T'_t + G_L H$$

where T'_t is the temperature at the dendrite tips. Thus, within the numerical domain, the temperature gradient in the liquid of the initial state is assumed to be linear. Notice that this initial state does not exactly match the steady-state thermal field, which is strictly obtainable only for an all-liquid zone of infinite height. Because we seek a nonlinear calculation for T, C, u, and w, it is not necessary that the initial state must match a steady state. However, we choose the values of C, T, and ϕ that rigorously match a steady state for the initial condition of the mushy zone.

C. *Boundary Conditions*

The domain is made finite by means of an artificial top boundary at $z' = z_t + H = 2H$ and by considering only the region $0 \le z \le 2H$.

The boundary condition associated with Eqs. [24] through [27] are as follows:

(1) No slip condition on velocities along the two vertical walls and the bottom boundary.
(2) No surface tractions at the top open boundary $z' = 2H$.

$$\sigma \cdot \mathbf{n} = 0$$

where $\mathbf{n}$ is the unit normal vector pointing outward from the boundary surface.
(3) Adiabatic vertical walls.
(4) Prescribed temperatures at bottom and top boundaries (with $z_t = H$):

$$T(x, 0, t) = \frac{T_E - T_0}{G_L H} \quad \text{and} \quad T(x, 2H, t) = \frac{T_t - T_0}{G_L H} + 1$$

(5) No solute flux at the vertical and bottom boundaries.
(6) At the top boundary, the solute must balance the concentration C_∞ outside; *viz.*, at the top boundary,

$$\frac{1}{\mathrm{Sc}} \frac{\partial C}{\partial z} + \sqrt{\frac{\mathrm{Ra}}{\mathrm{Pr}}} \hat{V} C = 0$$

(7) At the bottom, $z = 0$,

$$C = \frac{C_E - C_\infty}{C_\infty}$$

III. NUMERICAL METHOD

The governing Eqs. [23] through [27] have been discretized using a finite element method based on rectangular bilinear Lagrangian elements. The numerical model uses a Petrov-Galerkin formulation for convection-dominated transport and a penalty function approximation to impose incompressibility. The system of first-order ordinary differential equations in time resulting from the semidiscrete Petrov-Galerkin approximation is integrated using a generalized Newmark method.

The major features of the algorithm have been basically described in Heinrich[7] and Heinrich and Yu.[8] The detailed aspects of the method pertaining to a related solidification process can be found in Heinrich.[9]

A rectangular mesh has been used in all calculations with uniform nodal spacing in the x-direction but nonuniform in the vertical direction, where the mesh is heavily refined in the vicinity of the dendrite tips. The criteria for this refinement were (1) to allow a maximum change in the volume fraction liquid of no more than 7.5 pct between two consecutive nodes in the vicinity of the dendrite tips, where it changes very rapidly and (2) to place at least two nodal points within a distance D/V of the dendrite tips in the all-liquid region, to resolve the initial exponential decay in the solute concentration field. Finally, the changes in the mesh spacings in the z-direction were gradual, to avoid undesired mesh reflection effects.

IV. CALCULATED RESULTS FOR NONLINEAR CONVECTION

Calculations were performed for lead-tin systems under a variety of conditions. All calculations were started by introducing a random perturbation in the initial solutal field at the nodal points of the form

$$C(x, z, 0) = C_0(z)\,(1 + 0.005r) \qquad [28]$$

where $C_0(z)$ is the solutal concentration of the initial state and $-1 \le r \le 1$, with r taken from a random number generator.

Whether Eqs. [2] and [3] provide the most appropriate model for flow in the mushy zone is not yet definitive. A survey of the literature reveals that most authors differ in the form of the momentum transport equations in the mushy zone, in particular, in the coefficients for the transient, inertial, and viscous terms. Our formulation agrees with that of Beckermann and Viskanta.[10]

Chouhadry *et al.*[11] have shown that the convective inertial terms are negligible in a porous medium. However, the experimental work supporting this conclusion was for packed beds of spherical beads with $\phi \simeq 0.4$ and does not apply to the variable porosity case under consideration, in which $0 < \phi \le 1$. Our numerical results indicate a significant difference in the total kinetic energy of the flow in the mushy zone when the inertial terms are not included. Both models (with and without inertial terms) produce flow fields that are almost identical, but the one including the convective inertia terms shows consistently higher total kinetic energy in the mushy zone, and the difference stems from the flow close to the dendrite tips. This is consistent with the fact that the porosity approaches one at the tip of the dendrites.

The viscous terms in Eqs. [2] and [3], known as the Brinkman terms (*cf.* Brinkman[12]), are usually neglected when compared to the Darcy terms. These have the inconvenience that interface conditions must be imposed

at the tip of the dendrites,[13] which should not be necessary and is perhaps not valid when the porosity approaches unity. However, it is clear from experiments in packed beds that the Brinkman extension is appropriate when the porosity is greater than about 0.6, where the Darcy approximation is not a good model for the flow. A thorough discussion of the Brinkman term is given by Nield.[14] The exact form of this term, however, is not determined. It will depend on the form of the constitutive relation for the porous medium; moreover, it is sometimes recommended that the viscosity be interpreted as an "effective viscosity." In this work, the fluid viscosity μ has been used.

The most important changes in numerical results for the dendritic region are attributable to changes in the permeability function K. As we will see, the flow in the mushy zone is very sensitive to the values attained by K, and convection in the mushy zone can be eliminated if K is very small.

First, we discuss the result of nonlinear calculations for the Pb-20 wt pct Sn alloy, for which the linear stability analysis is presented in our companion paper.[5] The physical parameters are given in that reference, and only the nondimensional parameters will be mentioned here. Table I shows the different cases considered and the results of the linear stability analysis. The solidification velocity is 7.2 cm·h^{-1} (2×10^{-3} cm·s^{-1}) in all cases, and the upper boundary was chosen at $z' = 2H$.

Table I. Calculations for Pb-20 Wt Pct Sn

Calc. No.	Reference Thermal Gradient G_L (K·cm^{-1})	g/g_0 (g_0 = 980 cm·s^{-2})	Container Width (cm)	Linear Stability[5]
1	80	1	1.24	unstable
2	80	10^{-4}	1.24	stable
3	2.5	1	3.46	unstable
4	2.5	10^{-1}	3.46	unstable
5	2.5	10^{-2}	3.46	unstable
6	2.5	10^{-4}	3.46	stable
7	2.5	1	0.10	stable

In the case of $G_L = 80$ K·cm^{-1}, the depth of the dendritic region was found to be 1.24 cm, and when the gravitational constant is $g_0 = 980$ cm·s^{-2}, the nondimensional parameters are $Ra_T = 4.24 \times 10^4$, $Ra_C = 2.33 \times 10^7$, $Pr = 1.58 \times 10^{-2}$, $Sc = 91.0$, and $Da = 6.15 \times 10^{-8}\phi^3/(1 - \phi)$.

All of our nonlinear calculations agree with the linear stability results in the sense that when the stability analysis predicts an unstable case, convection develops in the nonlinear system, and when a stable system is predicted, the perturbations die out in the nonlinear model. In Figure 3, the results for calculation 1 after 114 seconds are shown. It can be observed that convection is very weak in the all-liquid region, and there is essentially no convection in the mushy zone. In fact, the permeabilities used in these calculations yield almost no convection in the mushy zone in all cases.

In the case $G_L = 2.5$ K·cm^{-1}, a depth of 17.3 cm results for the mushy zone, and at normal gravity conditions, the nondimensional parameters are $Ra_T = 4.97 \times 10^7$, $Ra_C = 6.28 \times 10^{10}$, and $Da = 2.75 \times 10^{-9}\phi^3/(1 - \phi)$ with the same values as before for the Prandtl and Schmidt numbers. Results at $t = 1080$ s for calculations 3 and 5 in Table I are shown in Figures 4 and 5, respectively. As expected, much weaker convection is observed in Figure 5 than in Figure 4 because of

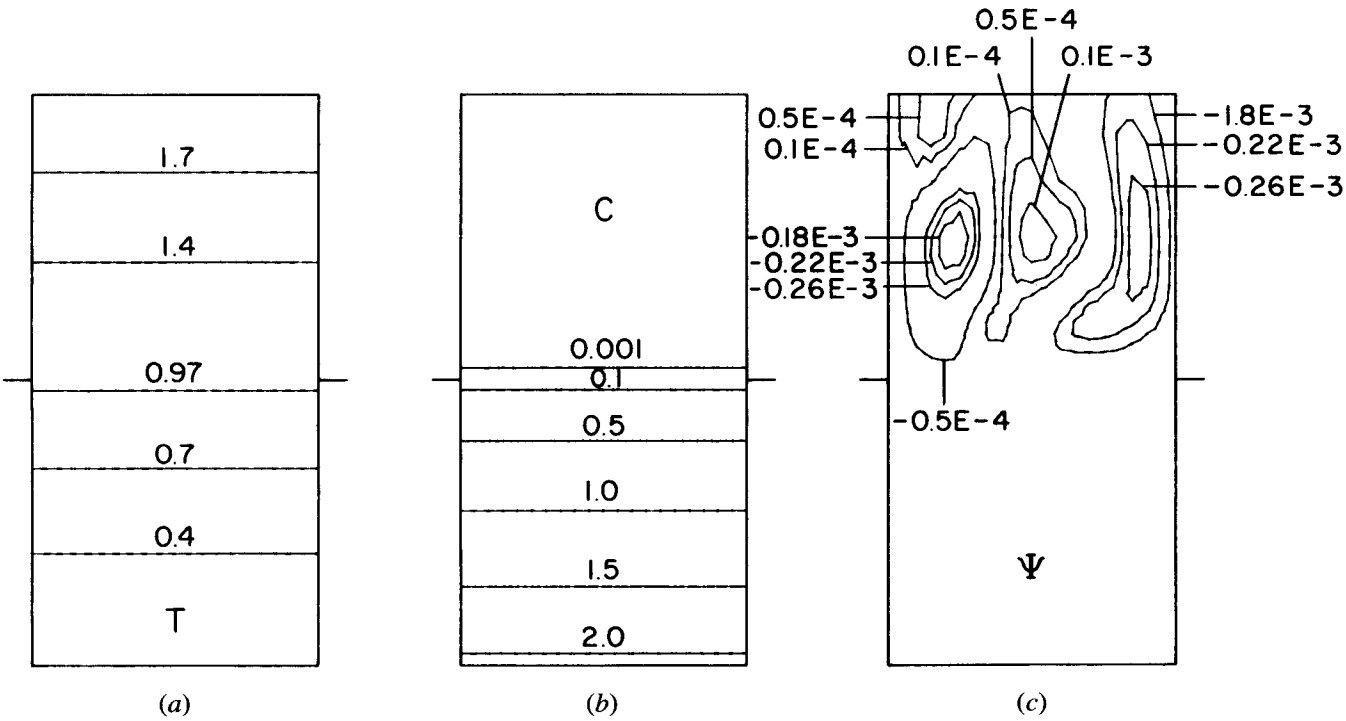

Fig. 3—Convection in a Pb-20 wt pct Sn alloy (calculation 1) at 114 s with $G_L = 80$ K·cm^{-1}. (*a*) Isotherms are $(T' - T_E)/(T_l - T_E)$, (*b*) solutal isoconcentrates, and (*c*) streamline contours.

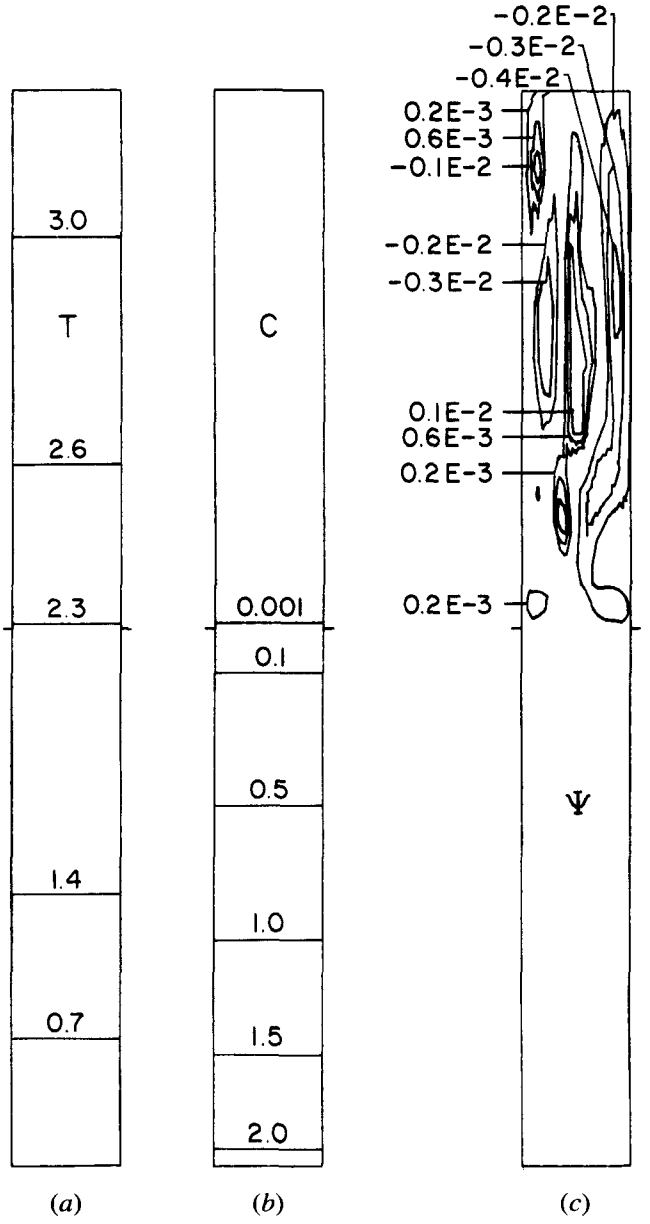

Fig. 4—Convection in a Pb-20 wt pct Sn alloy (calculation 3) at 1080 s with G_L = 2.5 K · cm^{-1}. (*a*) Isotherms are $(T' - T_E)/(T_l - T_E)$, (*b*) solutal isoconcentrates, and (*c*) streamline contours.

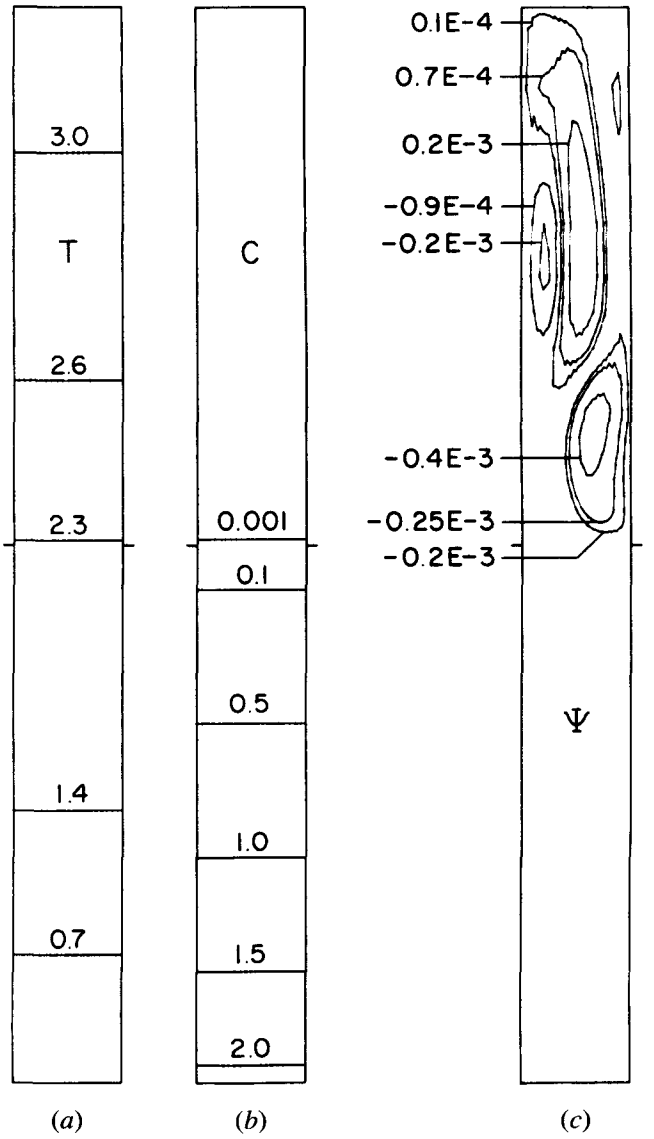

Fig. 5—Convection in the Pb-20 wt pct Sn alloy of Fig. 4 but at the reduced gravity 0.01 g_0 (calculation 5). (*a*) Isotherms are $(T' - T_E)/(T_l - T_E)$, (*b*) solutal isoconcentrates, and (*c*) streamline contours.

the reduced value of g. It can be observed that the convection cells in Figure 4 are much longer than those in Figure 3 because of the weaker stabilizing temperature gradient. These calculations show the expected results as predicted by the linear stability analysis of Nandapurkar *et al.*[5] However, these cases show no convection in the mushy zone and hardly any effect of thermosolutal convection in the conditions at the dendrite tips. We should point out that the linear stability calculations were done for laterally unbounded systems[5] and for values of g sufficiently high to cause convection. The systems were never found to be stable unconditionally for all wavelengths. Therefore, we have assumed that a system is stable provided that the linear analysis predicts stability for wavelengths equal to or greater than the width of the container.

Another series of calculations was performed for a Pb-10 wt pct Sn alloy at G_L = 50 K · cm^{-1} and a lower solidification velocity of 2.5 cm · h^{-1} (approximately 7 × 10^{-4} cm · s^{-1}). These are summarized in Table II.

The results for calculations 8 through 12 confirmed

Table II. Calculations for the Pb-10 Wt Pct Sn System

Calculation Number	Container Width (H = 2.4 cm)	g/g_0 (g_0 = 980 cm · s^{-2})	Linear Stability[5]
8	H	1	unstable
9	$2H$	1	unstable
10	$H/2$	1	unstable
11	$H/4$	1	unstable
12	$H/8$	1	unstable
13	$H/16$	1	stable
14	H	10^{-4}	stable

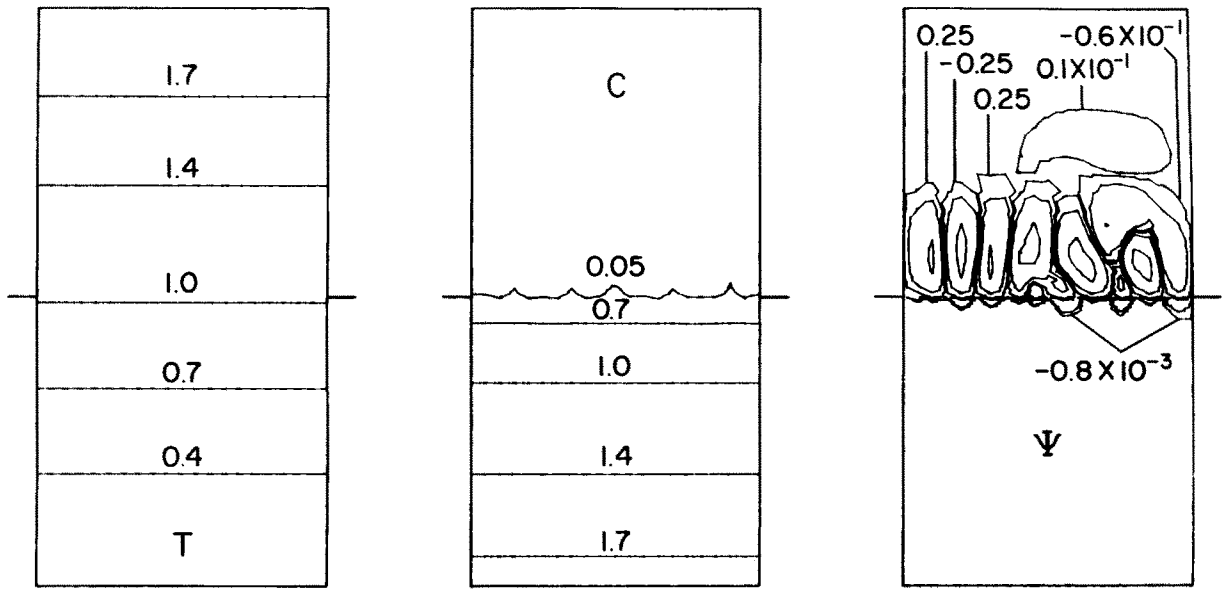

Fig. 6—Convection in a Pb-10 wt pct Sn alloy (calculation 8) at 700 s. (*a*) Isotherms are $(T - T_E)/(T_l - T_E)$, (*b*) solutal isoconcentrates, and (*c*) streamline contours.

that the size of the convection cells was independent of the width of the container. The depth of the mushy zone was $H = 2.4$ cm, and the top boundary was chosen at $z = 2H$. The parameters for these calculations, when the gravitational constant is g_0, are $Ra_T = 6.15 \times 10^5$, $Ra_C = 9.49 \times 10^7$, $Pr = 1.96 \times 10^{-2}$, $Sc = 82.3$, and $Da = 3.947 \times 10^{-7}\phi^3/(1 - \phi)$.

Results for calculation 8 in Table II are shown in Figure 6 at $t = 700$ s. It can be observed that, in this case, there is significant convection in the upper part of the mushy zone, and convection produces a strong disturbance in the concentration field at the tip of the dendrites. The temperature field remains virtually undisturbed. Note that dimensionless temperature is defined differently and given in the caption. Figure 7 shows a magnification close to the dendrite tips at 1887 seconds. A better organized cell system can be observed at this later time, and the effect of convection in the upper part of the dendrite region is evident. The temperature field has been magnified 100 times and shows how weakly it is affected by convection due to the very low Prandtl number. In all calculations performed so far, using values generally accepted for the Darcy number, convection in the mushy zone is only significant in the upper 20 pct of the dendritic region, if there is any convection at all. Furthermore, as can be observed in Figure 7(a), convection in the mushy zone is almost entirely driven by convection in the all-liquid region. This is more clearly illustrated by calculation 12 in Table II, for which the detail of the flow in the vicinity of the dendrite tips is depicted in Figure 8 at 1890 seconds. In all these figures, we should keep in mind that the streamline patterns obtained are not unique; they depend on the initial perturbations, and, hence, only the qualitative features of the flows are significant.

Further computations have been performed for this system for the parameters of calculation 8 in Table II but

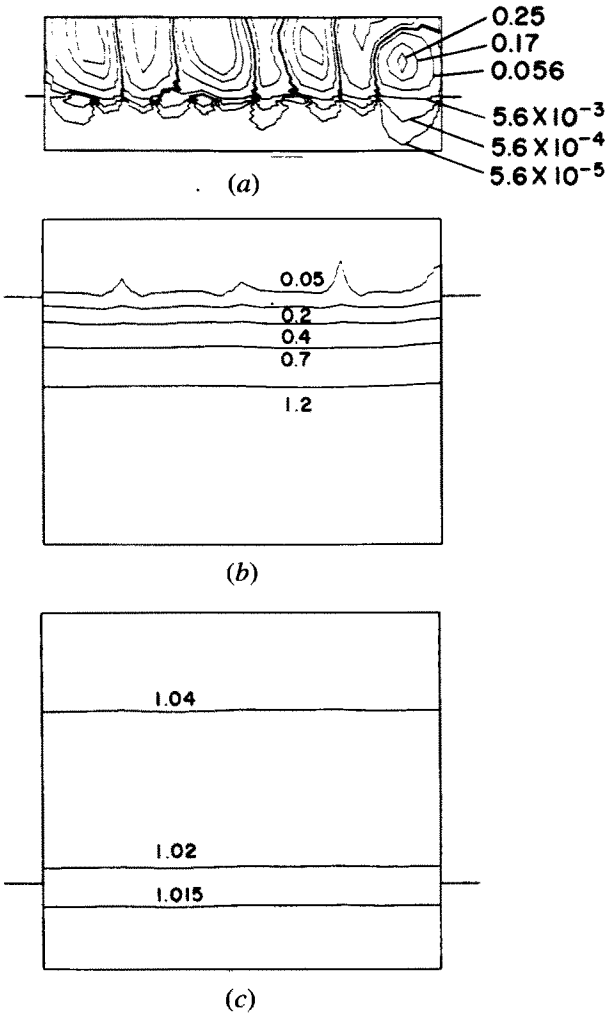

Fig. 7—Results for the same case of Fig. 6 magnified to show the effect of convection near the dendritic interface. (*a*) Isotherms, (*b*) solutal isoconcentrates, and (*c*) streamline contours.

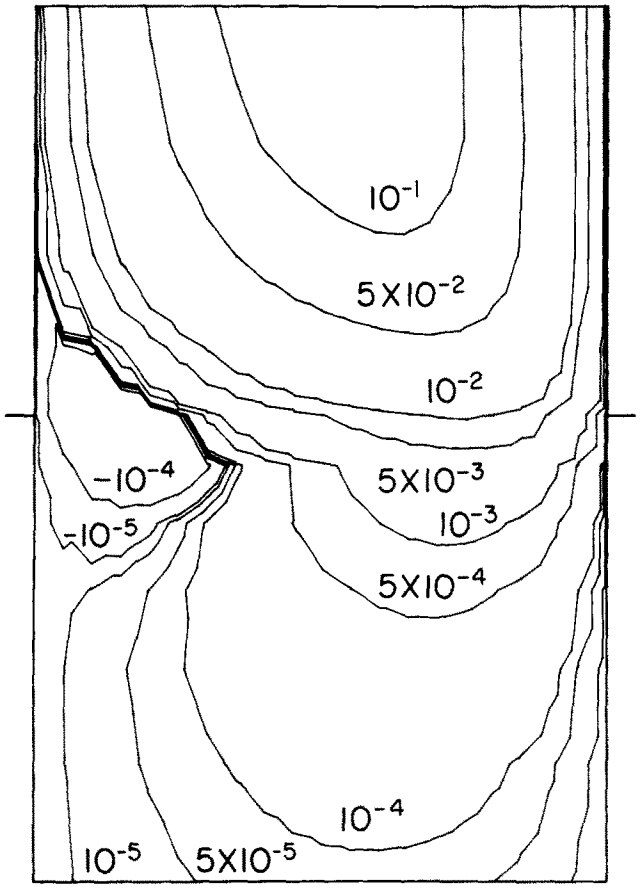

Fig. 8—Magnification of the flow field in calculation 12 (Table II) showing the streamlines near the dendritic interface.

with the gravitational vector oriented slightly off the negative vertical direction. Results show that very small deviations off the vertical direction produce a system entirely dominated by natural convection. The effect of both thermosolutal and natural convection could only be observed for deviations of up to 0.01 deg off the vertical direction. For a slightly larger angle of 0.05 deg, natural convection completely dominated the flow. These results have been reported elsewhere.[15]

V. CONCLUSIONS

Under the simplifying assumptions of steady-state solidification and that the tips of the dendrites describe a plane undeformable surface that advances at a constant velocity, nonlinear calculations of thermosolutal convection during vertical solidification of dendritic alloys have been performed. The model is an extension of the plane-front model analyzed by Coriell *et al.*[16] and McFadden *et al.*[17] to include a dendritic zone. The analysis shows significant differences when compared with the plane-front interface models, because of the presence of the mushy zone, in that the systems can be stable for higher solutal concentration values and were stable for all cases studied at a reduced gravity of 10^{-4} g_0. This suggests that the plane-front model is not relevant to solidification in the presence of a mushy zone.

The nonlinear calculations are in full agreement with the linear stability analysis presented in Nandapurkar *et al.*[5] and show that the presence of the mushy zone can have a stabilizing effect and suppress convection under low gravity conditions or when the lateral dimensions of the container are properly chosen. When the system is unstable, "fingerlike" convection develops in the all-liquid region that can entrain the interdendritic liquid in the mushy zone and significantly affect the solute concentration in the neighborhood of the tips of the dendrites. Furthermore, the calculated convection in the mushy zone under these conditions is always weak and very sensitive to the choice of the permeability function. For the permeability models used in this work, convection in the mushy zone never reached further than the upper 20 pct of the mushy zone and appeared to be driven mainly by convection in the all-liquid region.

It was also concluded that at gravity levels of 10^{-4} g_0, the Pb-Sn alloys considered were always stable to thermosolutal convection; moreover, when gravity is not acting exactly vertically, the presence of natural convection fully dominates the dynamics of the flow, under the conditions of this model.

The model presented here is only valid at the onset of convection. After some time, constitutional equilibrium is not satisfied, because it is assumed that the distribution of the volume fraction liquid remains constant with time. For this reason, calculations have been performed for a short time after the onset of convection that describe the main qualitative features of the dynamics of the flow in the vicinity of the dendrite tips. Extension of the present model to relax the condition—that the volumetric fraction of interdendritic liquid in the mushy zone is constant—is currently being pursued with the expectation that it will allow us to model the severe localized segregates in which remelting must take place, known as "channel segregates" or "freckles."

ACKNOWLEDGMENTS

The authors are grateful for the sponsorship of the Microgravity Sciences and Applications Division of NASA, Grant No. NAG 3 723. Discussions with V. Laxmanan, formerly of Case Western Reserve University, Cleveland, OH, and now of General Motors Research Laboratory, Warren, MI, A. Chait of NASA-LeRC, Cleveland, OH, A. Hellawell of Michigan Technological University, Houghton, MI, and S. Ganesan, K. Yeum, and A. Pearlstein of the University of Arizona, Tucson, AZ, on the general topic of convection associated with macrosegregation phenomena are greatly appreciated. One of the authors (DRP) also appreciates the partial support of the National Science Foundation, Grant No. MSM-8702732.

REFERENCES

1. V. Laxmanan, A. Studer, L. Wang, J.F. Wallace, and E.A. Winsa: *Gravitational Macrosegregation in Binary Pb-Sn Alloy Ingots*, NASA Technical Memorandum 89885, 1986.
2. J.R. Sarazin and A. Hellawell: *Metall. Trans. B*, 1988, vol. 19B, pp. 1861-71.
3. N. Streat and F. Weinberg: *Metall. Trans.*, 1974, vol. 5, pp. 2539-48.

4. M.C. Flemings: *Solidification Processing*, McGraw-Hill Book Co., New York, NY, 1974, pp. 247-48.
5. P. Nandapurkar, D.R. Poirier, J.C. Heinrich, and S. Felicelli: *Metall. Trans. B.*, 1989, vol. 20B, pp. 711-21.
6. D.R. Poirier: *Metall. Trans. B*, 1987, vol. 18B, pp. 245-55.
7. J.C. Heinrich: *Int. J. Numer. Meth. Eng.*, 1984, vol. 20, pp. 447-64.
8. J.C. Heinrich and C.-C. Yu: *Comput. Meth. Appl. Mech. Eng.*, 1988, vol. 69, pp. 1-27.
9. J.C. Heinrich: *Comput. Meth. Appl. Mech. Eng.*, 1988, vol. 69, pp. 65-88.
10. C. Beckermann and R. Viskanta: *Phys. Chem. Hydrodyn.*, 1988, vol. 10, pp. 195-213.
11. M. Chouhadry, M. Propster, and J. Szekely: *AIChE Journal*, 1976, vol. 22, pp. 600-03.
12. H.C. Brinkman: *Appl. Sci. Res.*, 1947, vol. A01, pp. 27-34.
13. G.S. Beavers and D.D. Joseph: *J. Fluid Mech.*, 1967, vol. 30, pp. 197-207.
14. D.A. Nield: *J. Fluid Mech.*, 1982, vol. 128, pp. 37-46.
15. J.C. Heinrich, S. Felicelli, P. Nandapurkar, and D.R. Poirier: Paper No. 89-0626, 27th AIAA Aerospace Science Meeting, Reno, NV, Jan. 8–12, 1988.
16. S.R. Coriell, M.R. Cordes, W.J. Boettinger, and R.F. Sekerka: *J. Cryst. Growth*, 1980, vol. 49, pp. 13-28.
17. G.B. McFadden, R.G. Rehm, S.R. Coriell, W. Chuck, and K.A. Morrish: *Metall. Trans. A*, 1984, vol. 15A, pp. 2125-37.